

## **DYNAMIC MODELING OF $\alpha$ IN THE ISOTROPIC LAGRANGIAN AVERAGED NAVIER-STOKES- $\alpha$ EQUATIONS**

**Hongwu Zhao\*** and **Kamran Mohseni** <sup>†</sup>  
Department of Aerospace Engineering Science  
University of Colorado at Boulder  
Boulder, Colorado 80309

**Jerrold E. Marsden** <sup>‡</sup>  
Control and Dynamical System  
California Institute of Technology  
Pasadena, CA 91125

### **ABSTRACT**

A *dynamic* procedure for the Lagrangian Averaged Navier-Stokes- $\alpha$  (LANS- $\alpha$ ) equations is developed where the variation in the parameter  $\alpha$  in the direction of anisotropy is determined in a self-consistent way from data contained in the simulation itself. In order to derive this model, the incompressible Navier-Stokes equations are Helmholtz-filtered at the grid and a test filter levels. A Germano type identity is derived by comparing the filtered subgrid scale stress terms with those given in the LANS- $\alpha$  equations. Assuming constant  $\alpha$  in homogenous directions of the flow and averaging in these directions, results in a nonlinear equation for the parameter  $\alpha$ , which determines the variation of  $\alpha$  in the non-homogeneous directions or in time. Consequently, the parameter  $\alpha$  is calculated during the simulation instead of a pre-defined value.

As an initial test, the dynamic LANS- $\alpha$  model is used to compute isotropic homogenous forced and decaying turbulence, where  $\alpha$  is constant over the computational domain, but is allowed to vary in time. The resulting simulations are compared with direct numerical simulations and with the LANS- $\alpha$  simulations using fixed value of  $\alpha$ . As expected,  $\alpha$  is found to change rapidly during the first eddy turn-over time during the simulations. It is also observed that by using the dynamic LANS- $\alpha$  procedure a more accurate simulation of the isotropic homogeneous turbulence is achieved. The energy spectra and the total kinetic energy decay are captured more accurately as compared

with the LANS- $\alpha$  simulations using a fixed  $\alpha$ . The current results suggest some promising applications of this dynamic LANS- $\alpha$  model, such as to a spatially varying turbulent flow, which we hope to undertake in future research.

### **NOMENCLATURE**

$L_{ij}$	Germano stress tensor
$p$	Pressure
$S_{ij}$	Strain tensor
$t$	Time
$\tau_{ij}$	Subgrid scale stress tensor with grid filter
$T_{ij}$	Subgrid scale stress tensor with test filter
$\mathbf{u}$	Velocity vector
$\alpha$	Modeling scale for LANS- $\alpha$ equation

### **INTRODUCTION**

Turbulent flows play an important role in many areas of engineering fluid mechanics as well as atmospheric and oceanic flows. Accurate simulation of a turbulent flow requires that the energetics of the large scale energy containing eddies, dissipative small scales, and inter-scale interactions to be accounted for. In direct numerical simulations (DNS) all the involved scales are directly calculated. DNS is believed to provide the most comprehensive representation of the governing equations of fluid flows; the so-called Navier-Stokes (NS) equations. Owing to the very high Reynolds numbers encountered in most problems of interest, the disparity between the large scales and small scales, which

\*Postdoctoral Research Associate, zhaoh@colorado.edu

<sup>†</sup>Assistant Professor, ASME member, mohseni@colorado.edu

<sup>‡</sup>Professor, marsden@cds.caltech.edu

represents the computational size of the problem, rapidly grows with the Reynolds number. Consequently, DNS can resolve only a small fraction of the turbulent activity for high Reynolds number flows.

While the direct numerical simulation of most engineering flows seems unlikely in near future, turbulence modeling could provide qualitative and in some cases quantitative measures for many applications. Large Eddy Simulations (LES) and the Reynolds Averaged Navier-Stokes Equations (RANS) are among the numerical techniques to reduce the computational intensity of turbulent calculations. In LES, the dynamics of the large turbulence length scales are simulated accurately and the small scales are modeled. The vast majority of contemporary LES make use of eddy-viscosity based Subgrid-Scale (SGS) models in conjunction with the spatially-averaged (filtered) Navier-Stokes Equations. In this approach, the effect of the unresolved turbulence is modeled as an effective increase in the molecular viscosity.

More recently, Holm, Marsden and their co-workers [1, 2] introduced a Lagrangian Averaging technique for modeling the mean flow of incompressible turbulent flows. Unlike the traditional averaging or filtering approach used for both RANS and LES, where the Navier-Stokes equation are averaged, the Lagrangian averaging approach is based on averaging at the level of the variational principle from which the Navier-Stokes equations are derived. That is, the Lagrangian Averaged Navier-Stokes equations for self-consistent mean fluid dynamics are derived by applying an averaging procedure to Hamilton's principle for an ideal incompressible fluid flow. The resulting mean fluid motion equation are obtained by using the Euler-Poincaré variational framework [1, 2]. As a result, these equations possess conservation laws for energy and momentum, as well as a Kelvin-type circulation theorem. Since the LANS- $\alpha$  equations are averaged over small spatial scales which are smaller than a pre-defined scale  $\alpha$ , the LANS- $\alpha$  simulations closely approximate the Navier-Stokes (NS) equations for scales larger than  $\alpha$ , while truncating the energy spectrum for scales smaller than  $\alpha$ . This averaging or filtering is done without adding physical viscosity, but by a nonlinear dispersion from the large scales. The numerical simulations of the LANS- $\alpha$  equations performed by Chen *et al* [3] and Mohseni *et al* [4] for isotropic homogenous turbulence has demonstrated that the LANS- $\alpha$  equations can accurately reproduce the large scales in a turbulent flow.

However, most engineering and geophysical flows of interest are often anisotropic. For example, due to rapid damping of turbulent fluctuations in the vicinity of a wall, the application of the isotropic LANS- $\alpha$  equations with a constant  $\alpha$  is not appropriate for long term calculations. In order to capture the correct behavior in such systems the parameter  $\alpha$  must be spatially or/and temporally varied in the direction of anisotropy [5], *i.e.* wall normal direction. There has been some attempt (with limited success) in order to remedy this problem. A successful *dynamic* LANS- $\alpha$  model is yet to be formulated and tested.

There are at least two approaches to anisotropy in the LANS- $\alpha$  equations:

- (i) To derive a set of *anisotropic* LANS- $\alpha$  equations. See alternative derivations in [6, 7].
- (ii) Use the isotropic LANS- $\alpha$  equations, but with a variable  $\alpha$  to compensate for the anisotropy.

At this point much more work must be done on the anisotropic LANS- $\alpha$  equations before they can be applied to practical problems. The second approach listed above is what will be explored in this study.

This paper is organized as follows: A dynamic LANS- $\alpha$  approach is proposed in next section where the variation in the parameter  $\alpha$  in the direction of anisotropy is determined in a self-consistent way from the data contained in the simulation itself. Our approach will be developed in the same spirit as the dynamic modeling procedure for conventional LES [8] which has achieved widespread use as very effective means of estimating model parameters as a function of space and time as the simulation progresses. The incompressible Navier-Stokes equations are Helmholtz-filtered at the grid and a test filter levels. A Germano type identity is derived by comparing the filtered subgrid scale stress terms with those given in the LANS- $\alpha$  equations. Considering a constant value of  $\alpha$  and averaging in the homogeneous directions of the flow results in a nonlinear equation for the parameter  $\alpha$ , which determines the variation of  $\alpha$  in the non-homogeneous directions or time. This nonlinear equation is solved by an iterative technique. Consequently, the parameter  $\alpha$  is calculated during the simulation instead of a fixed and pre-defined value. Numerical techniques for simulating the dynamic LANS- $\alpha$  model are described in the third section. The performance of the dynamic LANS- $\alpha$  model in simulating forced and decaying isotropic homogeneous turbulent flows are considered in the fourth section. Concluding results are presented in the last section.

## DERIVATION OF THE DYNAMIC LANS- $\alpha$ EQUATIONS

The LANS- $\alpha$  equations are given as follows (see [2, 9, 10] for a derivation)

$$\frac{\partial \mathbf{u}}{\partial t} + (\bar{\mathbf{u}} \cdot \nabla) \mathbf{u} - \alpha^2 (\nabla \bar{\mathbf{u}})^T \cdot \Delta \bar{\mathbf{u}} = -\nabla p + \frac{1}{Re} \Delta \mathbf{u} \quad (1)$$

where  $\bar{\mathbf{u}}$  is defined as

$$\bar{\mathbf{u}} = (1 - \alpha^2 \Delta)^{-1} \mathbf{u} \quad (2)$$

These equations are obtained by variational averaging of the Euler equation in Lagrangian representation over rapid fluctuations

whose amplitudes are of order  $\alpha$ . These equations can equivalently be represented by

$$\frac{\partial \bar{\mathbf{u}}}{\partial t} + (\bar{\mathbf{u}} \cdot \nabla) \bar{\mathbf{u}} = -\nabla \bar{p} + \frac{1}{Re} \Delta \bar{\mathbf{u}} - \nabla \cdot \boldsymbol{\tau}(\bar{\mathbf{u}}) \quad (3)$$

and the continuity equation

$$\nabla \cdot \bar{\mathbf{u}} = 0 \quad (4)$$

where  $\bar{p}$  is the modified pressure and  $\boldsymbol{\tau}(\bar{\mathbf{u}})$  is the subgrid scale stress tensor defined as

$$\boldsymbol{\tau}(\bar{\mathbf{u}}) = \alpha^2 (1 - \alpha^2 \Delta)^{-1} (\nabla \mathbf{u} \cdot \nabla \mathbf{u}^T - \nabla \mathbf{u}^T \cdot \nabla \mathbf{u} + \nabla \mathbf{u} \cdot \nabla \mathbf{u} + \nabla \mathbf{u}^T \cdot \nabla \mathbf{u}^T) \quad (5)$$

This subgrid scale stress is in fact the momentum flux of the large scales caused by the action of smaller, unresolved scales. It is known that the subgrid scale stress can also be derived by Helmholtz filtering the Navier-Stokes equations at a filtering length scale,  $\alpha$ , as we shall now explain.

We start with the incompressible NS equations,

$$\frac{\partial u_i}{\partial t} + u_j \frac{\partial u_i}{\partial x_j} = -\frac{\partial p}{\partial x_i} + \frac{1}{Re} \frac{\partial^2 u_i}{\partial x_j \partial x_j}. \quad (6)$$

Now define the following two filters associated with  $\alpha$  and  $\hat{\alpha}$ :

$$\bar{\mathbf{u}} = (1 - \alpha^2 \Delta)^{-1} \mathbf{u} \quad (7)$$

$$\widehat{\mathbf{u}} = (1 - \hat{\alpha}^2 \Delta)^{-1} (1 - \alpha^2 \Delta)^{-1} \mathbf{u} \quad (8)$$

For convenience, the first filter will be called the *grid filter*, while the second filter will be called the *test filter*. Applying these filters to equation (6) separately results in the following filtered equations

$$\frac{\partial \bar{u}_i}{\partial t} + \frac{\partial \bar{u}_i \bar{u}_j}{\partial x_j} = -\frac{\partial \bar{p}}{\partial x_i} + \frac{1}{Re} \frac{\partial^2 \bar{u}_i}{\partial x_j \partial x_j} - \frac{\partial \tau_{ij}}{\partial x_j} \quad (9)$$

and

$$\frac{\partial \widehat{u}_i}{\partial t} + \frac{\partial \widehat{u}_i \widehat{u}_j}{\partial x_j} = -\frac{\partial \widehat{p}}{\partial x_i} + \frac{1}{Re} \frac{\partial^2 \widehat{u}_i}{\partial x_j \partial x_j} - \frac{\partial T_{ij}}{\partial x_j}, \quad (10)$$

where

$$\tau_{ij} = \overline{u_i u_j} - \bar{u}_i \bar{u}_j \quad (11)$$

and

$$T_{ij} = \widehat{\overline{u_i u_j}} - \widehat{\bar{u}_i \bar{u}_j} \quad (12)$$

In analogy with the Germano identity [8], one can define

$$L_{ij} = T_{ij} - \widehat{\tau}_{ij} = \widehat{\overline{u_i u_j}} - \widehat{\bar{u}_i \bar{u}_j} \quad (13)$$

Next, we model the subgrid scale stresses under these two filtering actions by the LANS- $\alpha$  subgrid term in equation (5). That is, we set

$$\tau_{ij} = \alpha^2 (1 - \alpha^2 \Delta)^{-1} M_{ij} \quad (14)$$

and

$$T_{ij} = \hat{\alpha}^2 (1 - \hat{\alpha}^2 \Delta)^{-1} N_{ij}, \quad (15)$$

where

$$M_{ij} = \frac{\partial \bar{u}_i}{\partial x_k} \frac{\partial \bar{u}_j}{\partial x_k} - \frac{\partial \bar{u}_k}{\partial x_i} \frac{\partial \bar{u}_k}{\partial x_j} + \frac{\partial \bar{u}_i}{\partial x_k} \frac{\partial \bar{u}_k}{\partial x_j} + \frac{\partial \bar{u}_j}{\partial x_k} \frac{\partial \bar{u}_k}{\partial x_i} \quad (16)$$

and

$$N_{ij} = \frac{\partial \widehat{u}_i}{\partial x_k} \frac{\partial \widehat{u}_j}{\partial x_k} - \frac{\partial \widehat{u}_k}{\partial x_i} \frac{\partial \widehat{u}_k}{\partial x_j} + \frac{\partial \widehat{u}_i}{\partial x_k} \frac{\partial \widehat{u}_k}{\partial x_j} + \frac{\partial \widehat{u}_j}{\partial x_k} \frac{\partial \widehat{u}_k}{\partial x_i}. \quad (17)$$

Setting  $\hat{\alpha} = \beta \alpha$  and combining equations (13), (14) and (15) results in the following equation

$$L_{ij} = \beta^2 \alpha^2 (1 - \beta^2 \alpha^2 \Delta)^{-1} N_{ij} - \alpha^2 (1 - \beta^2 \alpha^2 \Delta)^{-1} (1 - \alpha^2 \Delta)^{-1} M_{ij}. \quad (18)$$

Writing above equation in a compact form results in

$$L_{ij} = \alpha^2 (\beta^2 \widehat{N}_{ij} - \widehat{M}_{ij}) \quad (19)$$

Multiplying  $S_{ij}$  on both sides of the above equation leads to

$$L_{ij} S_{ij} = \alpha^2 (\beta^2 \widehat{N}_{ij} - \widehat{M}_{ij}) S_{ij} \quad (20)$$

Next, take the spatial average of both sides of the above equation in the homogenous directions of the mean flow, which is denoted by the operation  $\langle \cdot \rangle$ , to obtain the following nonlinear equation for  $\alpha$

$$\alpha^2 = \frac{\langle L_{ij} S_{ij} \rangle}{\langle (\beta^2 \widehat{N}_{ij} - \widehat{M}_{ij}) S_{ij} \rangle} \quad (21)$$

where

$$S_{ij} = \frac{1}{2} \left( \frac{\partial \bar{u}_i}{\partial x_j} + \frac{\partial \bar{u}_j}{\partial x_i} \right) \quad (22)$$

The denominator in equation (21) could potentially approach zero, where it creates a singularity. In the dynamic LES, Lilly [11] used a least square approach to eliminate the singularity in Germano's model. If we apply a similar approach to equation (19), the following nonlinear equation for  $\alpha$  can be derived

$$\alpha^2 = F(\alpha) = \frac{\langle L_{ij} (\beta^2 \widehat{N}_{ij} - \widehat{M}_{ij}) \rangle}{\langle (\beta^2 \widehat{N}_{ij} - \widehat{M}_{ij}) (\beta^2 \widehat{N}_{ij} - \widehat{M}_{ij}) \rangle} \quad (23)$$

which does not have the singularity problem as in equation (21). This is a nonlinear equation for  $\alpha$ . All the quantities in equation (23) can be calculated during a LANS- $\alpha$  simulation. Therefore, equation (23) provides a nonlinear equation for dynamically calculating the value of  $\alpha$  during the simulation.

At this point the potential values for the free parameter  $\beta$  are required. In Fourier space, the grid and test filters can be expressed as

$$\check{\tilde{u}} = \frac{\check{u}}{1 + \alpha^2 k^2} \quad (24)$$

and

$$\begin{aligned} \check{\tilde{u}} &= \frac{\check{u}}{(1 + \beta^2 \alpha^2 k^2)(1 + \alpha^2 k^2)} \\ &\approx \frac{\check{u}}{1 + (\beta^2 + 1)\alpha^2 k^2} = \frac{\check{u}}{1 + \tilde{\alpha}^2 k^2} \end{aligned} \quad (25)$$

where  $\check{(\cdot)}$  stands for variables in the Fourier space,  $k$  is the wavenumber, and  $\tilde{\alpha}$  corresponds to filter scale for the test filter. Since  $\tilde{\alpha} = \sqrt{1 + \beta^2} \alpha \geq \alpha$ , one can realize that as long as  $\beta > 0$ , the test filter have a larger filter scale than the grid filter. Figure 1 shows the relative positions of the grid filter scale  $\alpha$  and the test

filter scale  $\tilde{\alpha}$  on a schematic of the energy spectrum for a high Reynolds number flow. In order to accurately model the subgrid scale stress, both the grid filter and the test filter scales must be located in the inertial sub-range of the energy spectrum.

The dynamic  $\alpha$  model given in equation (23) is designed to capture the length scale variations in space and time. Aside from the isotropic homogenous turbulent flows, it is well suited for anisotropic flows such as wall bounded turbulence or mixing flow turbulence, where the turbulence length scales could change in space or in time. In cases where there are directions of homogeneity, such as the streamwise and spanwise direction in a channel flow, one can average the parameter  $\alpha$  over the homogeneous directions. In a more general situation, we expect to replace the plane average, used in the channel flow, by an appropriate local spatial or time averaging scheme. For isotropic homogenous turbulence,  $\alpha$  is regarded as a constant in space and changes only in time.

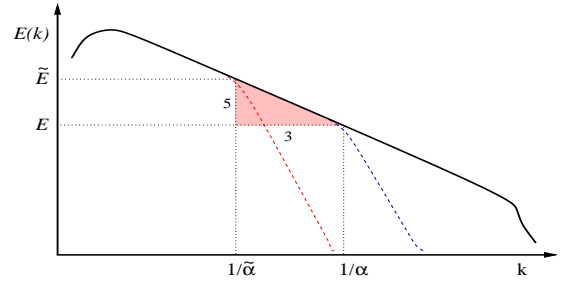


Figure 1. The relative positions of grid and test filter scales on the energy spectrum

## NUMERICAL METHOD

The numerical method used for the isotropic homogenous turbulence simulation in this study is based on a standard parallel pseudospectral scheme with periodic boundary conditions. The spatial derivatives are calculated in the Fourier domain, while the nonlinear convective terms are computed in the physical space. The flow fields are advanced in time in physical space using a fourth order Runge-Kutta scheme. To eliminate aliasing errors, the two-thirds rule is used so that the upper one third of each wave mode is discarded at each stage of the fourth order Runge-Kutta scheme.

We will focus on a isotropic homogenous turbulence simulation in a periodic cubic box of side  $2\pi$ . The initial flow field is chosen to be solenoidal, and the initial pressure fluctuations were obtained from the solution of the incompressible Poisson equation. The initial velocity field for each case was divergence

free and constructed from an energy spectrum of the form

$$E(k) \sim k^4 \exp[-2(k/k_p)^2] \quad (26)$$

The value of  $k_p$  corresponds to the peak in the energy spectrum.

For isotropic homogenous turbulence,  $\alpha$  in equations (21) and (23) is assumed to be only a function of time. The value of  $\alpha$  is obtained at the first stage of the Runge-Kutta integration at each time step by solving the nonlinear equation (23). This equation is solved by an iterative method. The solution is regarded as converged when the difference of  $\alpha$  values at two consecutive iterations is less than  $10^{-5}$ . Then the converged  $\alpha$  value is used for the SGS stress computation at the current time step and also is used as the initial value for the  $\alpha$  iteration at the next time step.

## RESULTS AND DISCUSSIONS

To test the capability of the dynamic LANS- $\alpha$  model in predicting the SGS stress, both decaying and forced isotropic homogenous turbulence simulations are investigated. The results using the dynamic  $\alpha$  model are compared with those using the fixed  $\alpha$  model as well as those by the direct numerical simulation. The LANS- $\alpha$  and dynamic LANS- $\alpha$  simulation are performed on a  $64^3$  grid, which corresponds to  $48^3$  after dealiasing, while the direct numerical simulation was performed on a  $128^3$  grid, which corresponds to  $85^3$  precision after dealiasing.

### Decaying case

In this simulation, we choose a decaying homogenous turbulence with initial Taylor Reynolds number  $Re_\lambda = 72$ , which corresponds to a computational Reynolds number of  $Re = 300$  and an initial energy spectrum peaked at  $k_p = 4$ . The eddy turn over time is about  $\tau = 0.9$ . Since the filter width aspect ratio,  $\bar{\alpha}/\alpha$ , which is the function of  $\beta$ , may influence the accuracy of the SGS stress modeling, it is necessary to discuss these effects and to find a proper range of  $\beta$  in equation (23).

In Figure 2, shows changes  $F(\alpha)$  and  $\alpha^2$  versus  $\alpha$  for various  $\beta$  values. The intersection points of the two curves are the roots of the equation  $\alpha^2 = F(\alpha)$ .  $F(\alpha)$  is computed with the initial velocity field since the existence of the roots for these equations at the initial time is essential for the nonlinear iteration at the subsequent time step. Figure 2(a) shows the roots of equation (23) and Figure 2(b) shows the roots of equation (21) with different  $\beta$  values at the initial time  $t = 0$ . It is seen that when  $\beta \leq 1$ , only one intersection point exists for curve  $\alpha^2$  and curve  $F(\alpha)$  on both figures, which means only one root exists for both equations (21) and equation (23). But when  $\beta > 1$ , two intersection points exist on Figure 2(a). One intersection point and one singularity point are observed on Figure 2(b). At the singularity point, the denominator has approached zero for equation (21) to make  $F(\alpha)$  become infinity. It is found that the first intersection

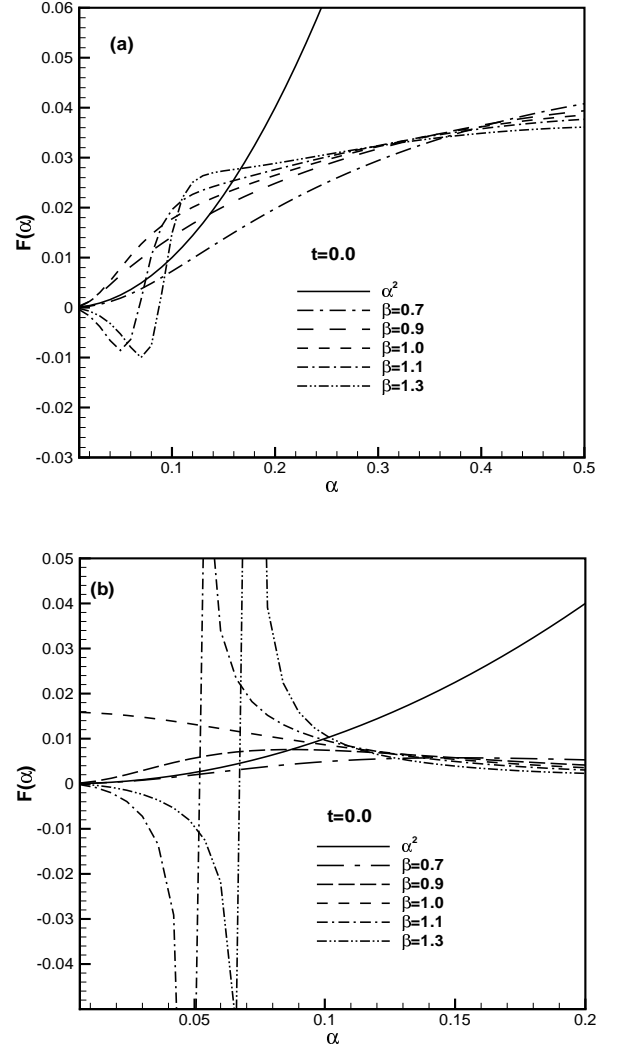


Figure 2. Effects of  $\beta$  on roots of equation  $\alpha^2 = F(\alpha)$  at  $t = 0.0$  for decaying case

point on Figure 2(a) corresponds to the singularity point on Figure 2(b). Therefore, this intersection point can not be regarded as a real root of equation (23). In solving the nonlinear equation (23), the initial value of  $\alpha$  should be chosen close to the second intersection point so that the value of  $\alpha$  can converge to this point. From Figure 2(a), it is also found that when the value of  $\beta$  is too small, such as  $\beta = 0.7$ , no root exists for equation (23). This is because, when the  $\alpha$  values in two filters are too close, the calculated resolved turbulent stress can be contaminated by numerical errors. On the other hand, if the value of  $\beta$  is too large, which means that two filters are too far away, the test filter may reach the energy containing eddy region. This implies that the

large energy-carrying scales are used to determine the contribution of subgrid scales. Thus, the equation (23) may not have a root or the converged  $\alpha$  value may not be accurate in modeling SGS stress. By trial and error for different flow parameters, it is found that when  $0.7 < \beta < 1.3$ , the equation (23) can coverage and thereby attain an appropriate uniquely determined  $\alpha$  value.

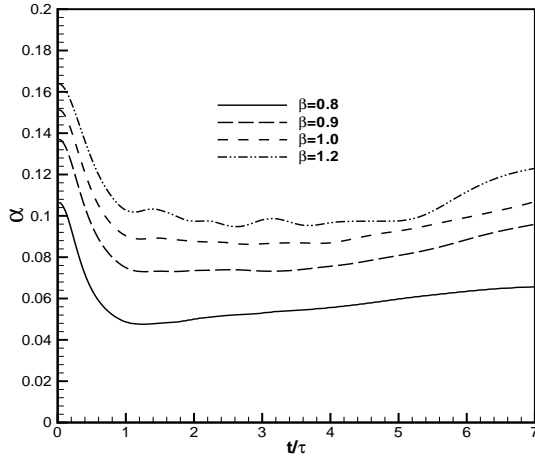


Figure 3. Time development of  $\alpha$  values at different  $\beta$  for decaying case:  $Re_\lambda = 72, \tau = 0.9$

Figure 3 and Figure 4 show the time development of  $\alpha$  value and the skewness  $\langle (\frac{\partial u}{\partial x})^3 \rangle / \langle (\frac{\partial u}{\partial x})^2 \rangle^{\frac{3}{2}}$  for  $\beta = 0.8 \sim 1.2$ . From the time development of skewness, it is observed that for this decaying turbulence, the energy cascade is built up at approximately one eddy turn over time. The skewness become flat after a quick transient period. Before the energy cascade is built up,  $\alpha$  experiences a sharp decreasing from a relatively large value at the initial time at all  $\beta$ . After approximately one eddy turn over time,  $\alpha$  reaches a relatively steady state and then undergoes a slow increase again after another 2 – 3 eddy turn over times. The fast increase of  $\alpha$  at later times is perhaps due to the lack of computational resolution. When the turbulence energy decays to a low level, the integral scales could grow to be comparable to the size of computational box.

Figure 5 shows the time evolution of the total kinetic energy and Figure 6 shows energy spectra at different times. The results with the dynamic  $\alpha$  model are compared with the DNS results for  $85^3$  grid resolution and LANS- $\alpha$  simulation results at  $\alpha = 0.15$ . While a slight dependency on the value of  $\beta$  is observed, in general, the energy spectrum at various times and the total kinetic energy decay are captured accurately. Mohseni *et al* [4] demon-

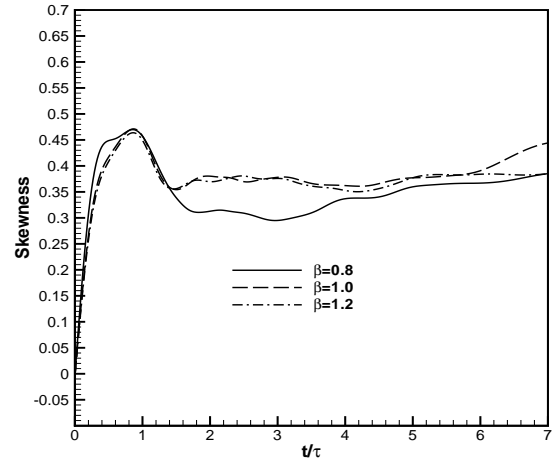


Figure 4. Time development of skewness at different  $\beta$  for decaying case:  $Re_\lambda = 72, \tau = 0.9$

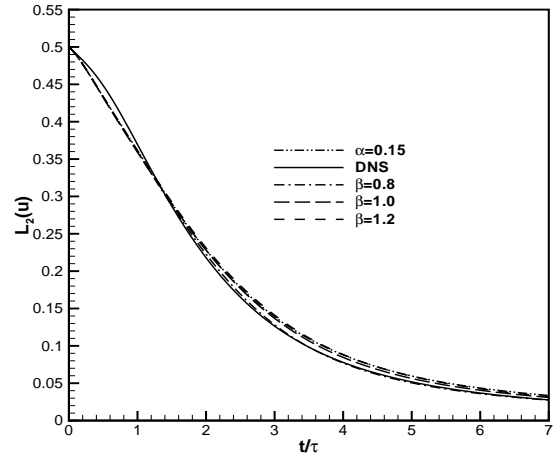


Figure 5. Time development of kinetic energy for decaying case:  $Re_\lambda = 72, \tau = 0.9$

strated that in order to accurately simulate a turbulent flow with the LANS- $\alpha$  equations, the value of  $\alpha$  should be somewhere, perhaps one decade lower than the peak of the energy spectra toward the grid resolution. Careful considerations of Figures 3 and 6 reveal that the dynamic LANS- $\alpha$  model of this study satisfies this criteria for all  $\beta$  values. In general, one expects that the value of  $\alpha$  to be in the inertial range of the energy spectra in order to

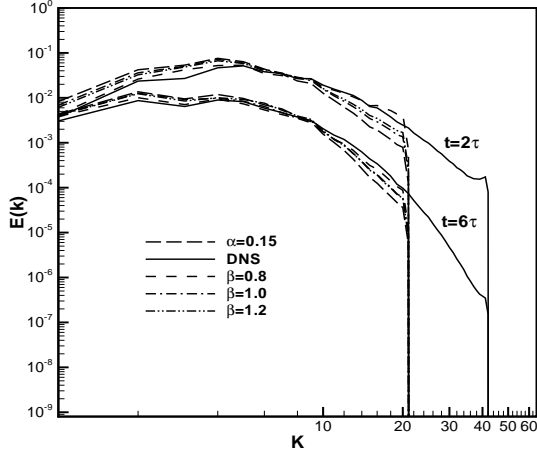


Figure 6. Energy spectra at  $t = 2\tau$  and  $t = 6\tau$  for decaying case

correctly capture the dynamics of the large scales. As illustrated in Figures 5 and 6, it is evident that the dynamic LANS- $\alpha$  model provides a better estimate of the total kinetic energy decay and the energy spectra over similar simulations with fixed  $\alpha$  calculations.

### Forced case

Forced isotropic turbulence in a periodic box can be considered as one of the most basic numerically simulated turbulent flows. Forced isotropic turbulence is achieved by applying isotropic forcing to low wave number modes so that the turbulent cascade develops as the statistical equilibrium is reached. Statistical equilibrium is signified by the balance between the input of kinetic energy through the forcing and its output through the viscous dissipation. The numerical forcing of a turbulent flow is usually referred to the artificial addition of energy to the large scale velocity components in the numerical simulation. In this study, we adopted a forcing method used in Chen *et al* [3] and Mosheni *et al* [4], where wave modes in a spherical shell  $|K| = k_0$  of a certain width are forced in such a way that the forcing spectrum follows Kolmogorov's  $-5/3$  scaling law

$$\tilde{f}_i = \frac{\delta}{N} \frac{\tilde{u}_i}{\sqrt{\tilde{u}_k \tilde{u}_k^*}} k^{-5/3}, \quad (27)$$

where  $\tilde{f}_i$  and  $\tilde{u}_i$  are the Fourier transforms of the forcing vector  $f_i$  and velocity  $u_i$ ,  $N$  is the number of wave modes that are forced, and  $\delta$  is the energy injection rate. This is done in order to obtain as long a range of near inertial behavior as possible. This type

of forcing ensures that the energy spectrum assumes the inertial range scaling starting from the lowest wave modes and thus an extended inertial range is artificially created. In the current run, we choose  $k_0 = 2$  and  $\delta = 0.1$ . The initial Taylor Reynolds number is  $Re_\lambda = 415$  and the initial energy spectrum is peaked at  $k_p = 1$ . The eddy turn over time is about  $\tau = 3.8$ .

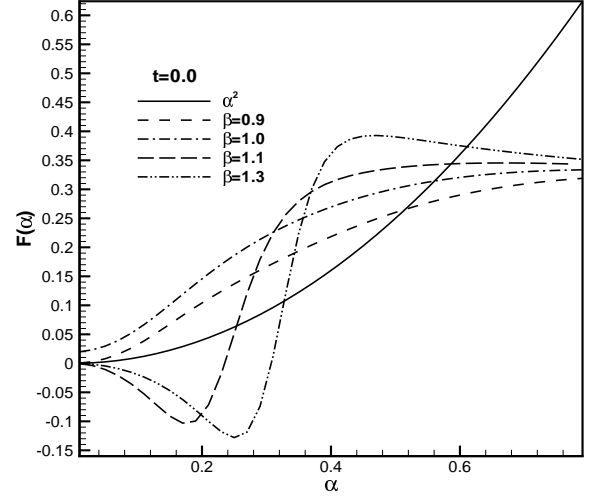


Figure 7. Effect of  $\beta$  on roots of equation  $\alpha^2 = F(\alpha)$  at  $t = 0$  for forced case

Figure 7 shows the influence of  $\beta$  values on the roots of equation (23) at the initial time  $t = 0$ . It is observed that for  $\beta \leq 1.0$ , only one root exists, while for  $\beta > 1.0$ , two roots exist for equation (23). As in the decaying case, the first root corresponds to the singularity point of equation (21). The  $\alpha$  value converged to this root can not be used for SGS stress computation. By numerical trial and error, the approximate range of applicable  $\beta$  values is found to be within  $0.7 < \beta < 1.1$  to obtain a correctly converged  $\alpha$  value at all time.

Figure 8 and Figure 9 show the time development of  $\alpha$  and skewness at  $\beta = 0.8$  and  $\beta = 1.0$ . Similar to decaying case, energy cascade is built up and the skewness reaches relatively steady after approximately 1 eddy turn over time for both  $\beta = 0.8$  and  $\beta = 1.0$ . A sharp decrease in the value of  $\alpha$  is observed over the first eddy turn over time, where the values of  $\alpha$  settles down toward a constant value. This corresponds to an statistically equilibrated state. As expected, the final value of  $\alpha$  is in the inertial range of the energy spectrum.

Figure 10 shows the evolution of the kinetic energy and Figure 11 shows the energy spectrum at  $t = 5.8\tau$  for  $\beta = 0.8$  and  $\beta = 1.0$ . An inertial subrange with  $\sim k^{-5/3}$  energy spectrum is

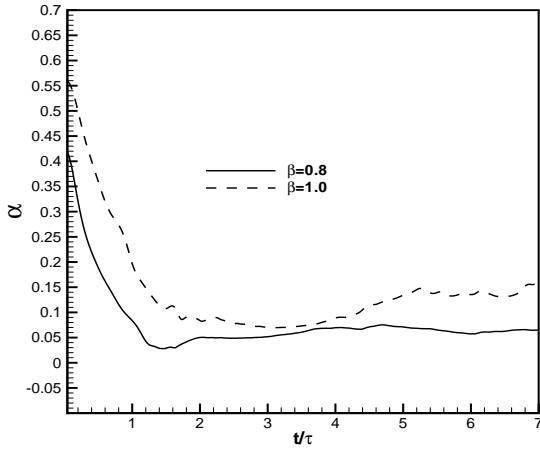


Figure 8. Time development of  $\alpha$  value at different  $\beta$  for forced case:  $Re_\lambda = 415, \tau = 3.8$

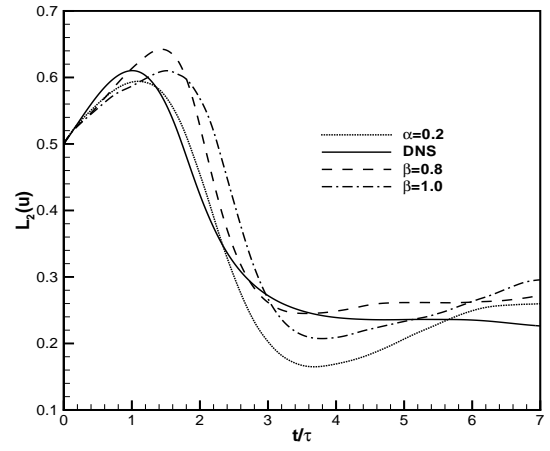


Figure 10. Time development of kinetic energy for forced case:  $Re_\lambda = 415, \tau = 3.8$

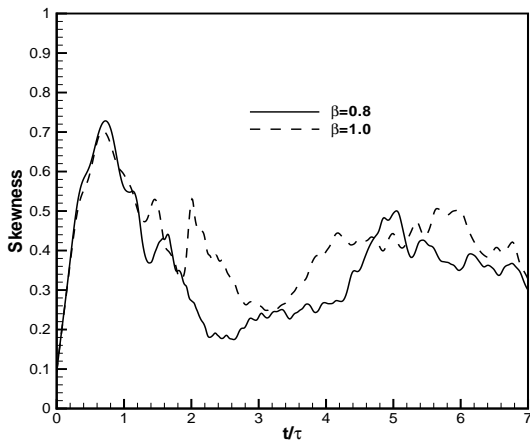


Figure 9. Time development of skewness at different  $\beta$  for forced case:  $Re_\lambda = 415, \tau = 3.8$

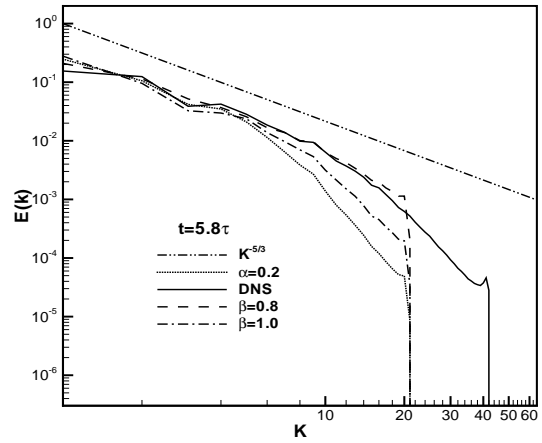


Figure 11. Energy spectrum at equilibrium status for forced case

evident in the dynamic LANS- $\alpha$  simulations. The results of the dynamic LANS- $\alpha$  simulations are compared with the DNS and the LANS- $\alpha$  simulations with  $\alpha = 0.2$ . The total kinetic energy decay and energy spectra of the dynamic LANS- $\alpha$  simulations for  $\beta = 0.8$  and  $1.0$  show a better agreement with the DNS data than those for a LANS- $\alpha$  simulation with a constant  $\alpha$ .

## CONCLUSIONS

In this paper, a dynamic LANS- $\alpha$  model is proposed and initial simulations are performed to test its capability. The model is derived based on a method similar to that used in the dynamic LES by using a Germano type identity. A nonlinear equation is obtained to dynamically compute an optimal  $\alpha$  by making use of the subgrid scale stress expression obtained from the LANS- $\alpha$  equations. The  $\alpha$  value is obtained by solving this nonlinear

equation iteratively. Numerical simulations were performed using the dynamic LANS- $\alpha$  model for both decaying and forced isotropic homogenous turbulence. The simulation results of both cases show that the computed  $\alpha$  values undergo a fast transient period during the first eddy turn-over time. After this transient period,  $\alpha$  reaches a relatively steady value. In the decaying case, after the turbulence total kinetic energy decays to a lower level,  $\alpha$  grows slowly as the integral length scale grow to a size comparable to the size of the computational domain. In the forced case,  $\alpha$  remains rather steady in time after the turbulence reaches an equilibrium status. The total kinetic energy decay rate and the energy spectra are predicted accurately by the dynamic LANS- $\alpha$  equations for both decaying and forced turbulence simulations. The energy spectrum and the decay of the total kinetic energy in a dynamic LANS- $\alpha$  simulation show a better agreement with the direct numerical simulation results than those obtained from the LANS- $\alpha$  model at a fixed value of  $\alpha$ . The current numerical simulations demonstrate that the application of the dynamic LANS- $\alpha$  model to anisotropic turbulence simulation is promising. Tests of our dynamic LANS- $\alpha$  model for wall bounded turbulent flows are planned in future investigations.

#### ACKNOWLEDGEMENT

The research in this paper was partially supported by the AFOSR contract F49620-02-1-0176. The authors would like to thank B. Kosovic for his initial help in the derivation of the dynamic model and T. Lund for helpful discussions.

#### REFERENCES

- [1] D. Holm, J. Marsden, and T. Ratiu. The Euler-Poincaré equations and semidirect products with application to continuum theories. *Adv. Math.*, 137:1, 1998.
- [2] D. Holm, J. Marsden, and T. Ratiu. Euler-Poincaré models of ideal fluids with nonlinear dispersion. *Phys. Rev. Lett.*, 80:4173, 1998.
- [3] S. Chen, D. Holm, L. Margoin, and R. Zhang. Direct numerical simulations of the Navier-Stokes alpha model. *Physica D*, 133:66, 1999.
- [4] K. Mohseni, B. Kosovic, S. Shkoller, and J. Marsden. Numerical simulations of the Lagrangian averaged Navier-Stokes equations for homogenous isotropic turbulence. *Physics of Fluids*, 15:524, 2003.
- [5] S.Y. Chen, C. Foias, D.D. Holm, E. Olson, E.S. Titi, and S. Wynne. Camassa-Holm equations as a closure model for turbulent channel and pipe flow. *Phys. Rev. Lett.*, 81:5338–5341, 1998.
- [6] D.D. Holm. Fluctuation effects on 3D Lagrangian mean and Eulerian mean fluid motion. *Physica D.*, 133:215–269, 1999.
- [7] J.E. Marsden and S. Shkoller. The anisotropic Lagrangian

averaged Euler and Navier-Stokes equations. *Arch. Rational Mech. Anal.*, 166(27-46):27–46, 2002.

- [8] M. Germano, U. Piomelli, P. Moin, and W. Cabot. A dynamic subgrid-scale eddy viscosity model. *Physics of Fluids A*, 3(7):1760, 1991.
- [9] D. Holm. Fluctuation effects on 3D Lagrangian mean and Eulerian mean fluid motion. *Physica D*, 133:215, 1999.
- [10] H. S. Bhat, R. C. Fetecau, J. E. Marsden, K. Mohseni, and M. West. Lagrangian averaging for compressible fluids. *to appear in the SIAM Journal on Multiscale Modeling and Simulation*, 2004. Also <http://arxiv.org/abs/physics/0311086>.
- [11] D. Lilly. A proposed modification of the Germano subgrid-scale closure method. *Physics of Fluids A*, 4(3):633, 1992.